Published in final edited form as:

Ophthalmology. 2019 April ; 126(4): 565–575. doi:10.1016/j.ophtha.2018.11.015.

DeepSeeNet: A deep learning model for automated classification of patient-based age-related macular degeneration severity from color fundus photographs

Yifan Peng, PhD[#1], **Shazia Dharssi**[#1,2], **Qingyu Chen, PhD**[1], **Tiarnan D. Keenan, BM BCh, PhD**[2], **Elvira Agrón, MS**[2], **Wai T. Wong, MD**[2], **Emily Y. Chew, MD**[2], and **Zhiyong Lu, PhD**[1]

[1.]National Center for Biotechnology Information (NCBI), National Library of Medicine (NLM), National Institutes of Health (NIH), Bethesda, Maryland, United States;

[2.]National Eye Institute (NEI), National Institutes of Health (NIH), Bethesda, Maryland, United States;

[#] These authors contributed equally to this work.

Abstract

Purpose: In assessing the severity of age-related macular degeneration (AMD), the Age-Related Eye Disease Study (AREDS) Simplified Severity Scale predicts the risk of progression to late AMD. However, its manual use requires the time-consuming participation of expert practitioners. While several automated deep learning (DL) systems have been developed for classifying color fundus photographs of individual eyes by AREDS severity score, none to date has utilized a patient-based scoring system that employs images from both eyes to assign a severity score.

Design: DeepSeeNet, a DL model, was developed to classify patients automatically by the AREDS Simplified Severity Scale (score 0-5) using bilateral color fundus images.

Participants: DeepSeeNet was trained on 58,402 and tested on 900 images from the longitudinal follow up of 4,549 participants from AREDS. Gold standard labels were obtained using reading center grades.

Corresponding Author(s) Emily Y. Chew, MD, National Eye Institute (NEI), National Institutes of Health (NIH), 9000 Rockville Pike, Bethesda, Maryland, United States, echew@nei.nih.gov, 301.496.6583, Zhiyong Lu, PhD, National Center for Biotechnology Information, National Library of Medicine, National Institutes of Health, 9000 Rockville Pike, Bethesda, MD 20894. zhiyong.lu@nih.gov.

Authorship:
Conception and design: Peng, Dharssi, Chew, Lu
Analysis and interpretation: Peng, Dharssi, Chen, Keenan, Agron, Wong, Chew, Lu
Data collection: Peng, Dharssi, Chen, Agron, Wong, Chew
Drafting the work: Peng, Dharssi, Chen, Keenan, Wong, Chew, Lu

Conflict of Interest: no conflicting relationship exists for any author

Online Supplemental Materials: This article contains additional online-only material. The following should appear online-only: Figures S1, S2, and S3, S4, Tables S1 and S2, S3, and Training strategies.

Publisher's Disclaimer: This is a PDF file of an unedited manuscript that has been accepted for publication. As a service to our customers we are providing this early version of the manuscript. The manuscript will undergo copyediting, typesetting, and review of the resulting proof before it is published in its final citable form. Please note that during the production process errors may be discovered which could affect the content, and all legal disclaimers that apply to the journal pertain.

Methods: DeepSeeNet (composed of three sub-networks) simulates the human grading process by first detecting individual AMD risk factors (drusen size; pigmentary abnormalities) for each eye and then calculating a patient-based AMD severity score using the AREDS Simplified Severity Scale.

Main Outcome Measures: Overall accuracy, specificity, sensitivity, Cohen's kappa, area under the curve (AUC). The performance of DeepSeeNet was compared to that of retinal specialists.

Results: DeepSeeNet performed better on patient-based, multi-class classification (accuracy=0.671; kappa=0.558) than retinal specialists (accuracy=0.599; kappa=0.467) with high AUCs in the detection of large drusen (0.94), pigmentary abnormalities (0.93) and late AMD (0.97), respectively. DeepSeeNet also outperformed retinal specialists in the detection of large drusen (accuracy 0.742 vs 0.696; kappa 0.601 vs 0.517) and pigmentary abnormalities (accuracy 0.890 vs 0.813; kappa 0.723 vs 0.535) but showed lower performance in the detection of late AMD (accuracy 0.967 vs 0.973; kappa 0.663 vs 0.754).

Conclusions: By simulating the human grading process, DeepSeeNet demonstrated high accuracy with increased transparency in the automated assignment of individual patients to AMD risk categories based on the AREDS Simplified Severity Scale. These results highlight the potential of deep learning systems to assist and enhance clinical decision-making processes in AMD patients such as early AMD detection and risk prediction for developing late AMD. DeepSeeNet is publicly available on https://github.com/ncbi-nlp/DeepSeeNet.

Keywords

deep learning; age-related macular degeneration (AMD); Age-Related Eye Disease Study (AREDS); convolutional neural network (CNN); artificial intelligence (AI)

Age-related macular degeneration (AMD) is responsible for approximately 9% of global blindness and is the leading cause of visual loss in developed countries[1,2]. The number of people with AMD worldwide is projected to be 196 million in 2020, rising substantially to 288 million in 2040[3]. The prevalence of AMD increases exponentially with age: late AMD in white populations has been estimated by meta-analysis at 6% at 80 years and 20% at 90 years[4]. Over time, increased disease prevalence through changing population demographics may place great burdens on eye services, especially where retinal specialists are not available in sufficient numbers to perform individual examinations on all patients. It is conceivable that deep learning and/or telemedicine approaches might support future eye services; however, this might only apply when evidence-based systems have undergone extensive validation and demonstrated performance metrics that are at least non-inferior to those of clinical ophthalmologists in routine practice.

AMD arises from a complex interplay between aging, genetics, and environmental risk factors[5,6]. It is regarded as a progressive, step-wise disease, and is classified by clinical features (based on clinical examination or color fundus photography) into early, intermediate, and late stages[7]. The hallmarks of intermediate disease are the presence of large drusen and/or pigmentary abnormalities at the macula. There are two forms of late AMD: (1) neovascular AMD, and (2) atrophic AMD, with geographic atrophy (GA).

The Age-Related Eye Disease Study (AREDS), sponsored by the National Eye Institute (National Institutes of Health), was a randomized clinical trial to assess the effects of oral supplementation with antioxidant vitamins and minerals on the clinical course of AMD and age-related cataract. Longitudinal analysis of this study cohort led to the development of the patient-based AREDS Simplified Severity Scale for AMD, based on color fundus photographs[8]. This simplified scale provides convenient risk factors for the development of advanced AMD that can be determined by clinical examination or by less demanding photographic procedures than used in the Age-Related Eye Disease Study. The scale combines risk factors from both eyes to generate an overall score for the individual, based on the presence of one or more large drusen (diameter >125 μm) and/or AMD pigmentary abnormalities at the macula of each eye[8]. The Simplified Severity Scale is also clinically useful, in that it allows ophthalmologists to predict an individual's 5-year risk of developing late AMD. This 5-step scale (from score 0 to 4) estimates the 5-year risk of the development of late AMD in at least one eye as 0.4%, 3.1%, 11.8%, 25.9%, and 47.3%, respectively[8].

Automated image analysis tools have demonstrated promising results in biology and medicine[9-15]. In particular, deep learning, a subfield of machine learning, has recently generated substantial interest in the field of ophthalmology[9,16-21]. Past studies have utilized deep learning systems for the identification of various retinal diseases, including diabetic retinopathy [22-27] glaucoma [27-30] retinopathy of prematurity [31], and AMD [19,21,27,32,33] In general, deep learning is the process of training algorithmic models with labeled data (e.g. color fundus photographs categorized manually as containing pigmentary abnormalities or not), where these models can then be used to assign labels automatically to new data. Deep learning differs from traditional machine learning methods in that specific image features do not need to be pre-specified by experts in that field. Instead, the image features are learned directly from the images themselves.

Recently, several deep learning systems have been developed for the classification of color fundus photographs into AMD severity scales, at the level of the individual eye. These severity scales have included both binary (e.g. referable vs. non-referable AMD[17,19,21,27,32]) and multi-class (e.g. the 9-step AREDS Severity Scale[16,34] and a 4-class AMD classification[35]) systems. However, to the best of our knowledge, none to date has developed a patient-based system that, similar to the AREDS Simplified Severity Scale score, uses images from both eyes to obtain one overall score for the individual. This is particularly relevant because estimates of rates of progression to late AMD are highly influenced by the status of fellow eyes, as the behavior of the two eyes is highly correlated[8]. Additionally, several recent studies have reported robust performance in the automated classification of AMD from OCT scans[21,36-39]. Unlike these studies, DeepSeeNet is based on data from color fundus photography, which remains an important imaging modality for assessing the involvement of retinal and choroidal blood vessels in ophthalmic disease, and is essential in grading eyes using the AREDS Simplified Severity Score[40]. Similar to De Fauw et al[37], DeepSeeNet contains two stages by design for improved performance and increased transparency. However, their two-stage approach is different from ours with respect to the actual approach details as well as issues in data variability.

The primary aim of our study was to train and test a deep learning model to identify patient-level AMD severity using the AREDS Simplified Severity Scale from color fundus images of both eyes. Images were obtained from the AREDS dataset, one of the largest available datasets containing nearly 60,000 retinal images. Different from previous methods, our proposed model mimics the human grading process by first detecting individual risk factors (drusen and pigmentary abnormalities) in each eye and then combining values from both eyes to develop an AMD score for the patient. Hence, our model closely matches the clinical decision-making process, which allows an ophthalmologist to inspect and visualize an interpretable result, rather than being presented with an AMD score by a 'black-box' approach. This approach offers potential insights into the decision-making process, in a fashion more typical of clinical practice, and has the advantages of transparency and explainability.

Methods and Materials

The specific aims of the study were: (1) to compare the performance of three deep learning models generated by three different training strategies; (2) for the most accurate of these three models, to compare its performance with that of retinal specialists (AREDS investigators whose assessments had previously been recorded during the AREDS).

The reference measure used as the "gold standard" for both training purposes and the measurement of performance was the grading previously assigned to each color fundus photograph by human graders at the Reading Center for the AREDS, as described below.

Assignment of the AREDS Simplified Severity Scale by Reading Center grading

This study employed the AREDS dataset[8]. Briefly, the AREDS was a 12-year multi-center, prospective cohort study of the clinical course, prognosis, and risk factors of AMD and age-related cataract. Institutional review board approvals were obtained from each of the 11 clinical sites and written informed consents were obtained from each of the AREDS study participants. Stereoscopic color fundus photographs from both eyes (field 2, 30° imaging field centered at the fovea) were obtained at the study baseline, the 2-year follow-up visit, and annually thereafter. Due to inherent redundancy in a pair of stereoscopic photographs, for each eye, only one of the pair of photographs was used in the current study. In general, the left image of the pair was used unless missing from the database, in which the right image was utilized instead (~0.5%).

The gold standard annotation (image labeling) was performed by expert human graders at the Reading Center (University of Wisconsin). The workflow is described in detail in AREDS Report number 6[41]. In brief, a senior grader (grader 1) performed preliminary grading of the photograph for AMD severity using a standardized protocol for a 4-category scale and a junior grader (grader 2) performed detailed grading of the photograph for multiple specific AMD features. A computerized algorithm then extracted the AMD severity levels from the detailed gradings (by grader 2). In the case of any discrepancy regarding the AMD severity level between the graders, a senior investigator would adjudicate the final severity level. All photographs were graded independently, i.e. graders were masked to the photographs and grades from previous visits. Senior graders had around 10-15 years of experience and junior graders had up to 5 years of experience.

In addition, a rigorous process of grading quality control was performed at the Reading Center including the assessment for the inter-grader and intra-grader agreement overall and according to specific AMD features.[41]. Analyses for potential ‘temporal drift’ was conducted by having all graders regrade in a masked fashion the same group of images annually for the duration of the study.

For each participant, at each time-point, grades for both eyes were employed to calculate the AREDS Simplified Severity Scale score. This scale ranges from 0 to 5, with a score of 0 to 4 assigned to participants based on the drusen/pigment status in each eye, and a score of 5 assigned to participants with late AMD (defined as either neovascular AMD or central GA) in either eye (Figure 1). This is a modification of the original scoring method described in Ferris et al[8]. As described above, these scores were used as gold standard labels (i.e., reference), both for training purposes and to assess the performance of the different models developed in this study.

Image datasets used in the training and testing of the deep learning model

The AREDS dataset is publicly accessible to researchers by request at dbGAP (https://www.ncbi.nlm.nih.gov/projects/gap/cgi-bin/study.cgi?study_id=phs000001.v3.p1) [8]. A total of 59,302 color fundus images from 4,549 participants were extracted from the AREDS dataset. This dataset was divided into two subsets: (1) a testing dataset, which consisted of bilateral images captured at the study baseline from 450 participants (i.e. one image from each eye); at the time of the study, in addition to undergoing normal Reading Center grading, these images were also assessed (separately and independently) by the retinal specialists, whose responses were recorded; and (2) a training dataset, which consisted of 58,402 images from the remaining 4,099 participants, captured at multiple study visits (though not all participants had follow-up visits through to 12 years). The images taken from the group of 450 participants at visits other than the baseline visit were not used in either dataset (Figure S1, available at www.aaojournal.org). Table 1 summarizes the distribution of participants by the AREDS Simplified Severity Scale at baseline. Table 2 summarizes the distributions of scored AMD features among the training and testing datasets.

Composition of the DeepSeeNet deep learning model

DeepSeeNet was designed as a deep learning model that could be used to assign patient-based AREDS Simplified Severity Scale scores in an automated manner using bilateral color fundus photographs (Figure S3, available at www.aaojournal.org). DeepSeeNet simulates the grading process of ophthalmologists by first detecting the presence or absence of AMD risk-associated features for each eye (large drusen and AMD pigmentary abnormalities) and then using this bilateral data to compute a patient-based score (0-5) using the algorithm described above.

DeepSeeNet consists of three constituent parts that contribute to its output: (a) a sub-network, Drusen-Net (D-Net), which detects drusen in three size categories (small/none, medium, and large); (b) a sub-network, Pigment-Net (P-Net), which detects the presence or absence of pigmentary abnormalities (hypopigmentation or hyperpigmentation); and (c) a sub-network, Late AMD-Net (LA-Net), which detects the presence or absence of late AMD (neovascular AMD or central GA).

D-Net, P-Net, and LA-Net were designed as deep convolutional neural networks (CNNs)[42], each with an Inception-v3 architecture[43], which is a state-of-the-art CNN model for image classification. In total, there are 317 layers in the Inception-v3 model, comprising a total of >21 million weights (learnable parameters) that were subject to training.

Prior to training, we followed the lead of Burlina et al[18,35] to preprocess our image data as follows: the AREDS fundus photographs were cropped to generate a square image field encompassing the macula, followed by scaling the image to a resolution of 224×224 pixels (Figure S2, available at www.aaojournal.org). We trained our model in Keras with TensorFlow as the backend[44,45]. During the training process, we updated the model parameters using the Adam optimizer (learning rate of 0.0001) for every minibatch of 32 images[46]. This reduces the variance of the parameter update, which leads to a more stable convergence. The training was stopped after 5 epochs (passes of the entire training set) once the accuracy values no longer increased or started to decrease. All experiments were conducted on a server with 32 Intel Xeon CPUs, using a wNVIDIA GeForce GTX 1080 Ti 11Gb GPU for training and testing, with 512Gb available in RAM memory.

Performance comparison between DeepSeeNet and retinal specialists

We compare the performance of the deep learning model with that of retinal specialists, using the Reading Center grades as the gold standard, in both cases. For the performance of the retinal specialists, we used the AREDS Simplified Severity Scale scores that had previously been recorded from the retinal specialists who originally served as the AREDS investigators. These scores were recorded at the AREDS baseline study visits, when the retinal specialists (n = 88) had independently assessed 450 AREDS participants as part of a qualification survey used to determine initial AMD severity for each eye. The clinical assessment involved the determination of the following features: drusen size (within 2-disc diameter of macula center), presence of pigmentary abnormalities consistent with AMD (within 1-disc diameter), AMD subretinal neovascularization (SRNV), previous laser photocoagulation for AMD SRNV, central GA, retinal pigment epithelial detachment, and disciform scar. These clinical assessments were employed to derive the same patient-based Simplified Severity Scale as defined in Figure 1.

Overall accuracy, specificity, sensitivity, Cohen's kappa[47,48], and receiver operating characteristic curve analysis were used to evaluate the performance of DeepSeeNet and retinal specialists (with reference to the Reading Center grades as the gold standard). The kappa values < 0 indicate no agreement, and 0-0.20 indicate slight, 0.21-0.40 fair, 0.41-0.60 moderate, 0.61-0.80 as substantial, and 0.81-1 almost perfect agreement[49]. We also followed the work of Poplin et al. to assess the statistical significance of the results[50]. For the test dataset, we sampled 450 patients with replacement and evaluated the model on this sample. By repeating this sampling and evaluation 2,000 times, we obtained a distribution of the performance metric (such as Kappa) and reported 95% confidence intervals.

Results

Predicting AREDS simplified severity scale

DeepSeeNet predicted AREDS Simplified Severity Scale scores for each participant in the testing dataset (n=450). The performance of the deep learning models was measured against the Reading Center grades previously assigned to these 450 participants (as the reference or gold standard).

We investigated three strategies for training and optimizing DeepSeeNet (details located under ‘Training strategies’ in supplementary materials, available at www.aaojournal.org) and found the fine-tuning strategy (all layers in a pre-trained Inception-v3 model were fine-tuned using the AREDS dataset) achieved the best results, with accuracy=0.67 and kappa=0.56. As a result, we will only discuss Fine-tuned DeepSeeNet hereafter.

The performance of Fine-tuned DeepSeeNet was then compared with that of the retinal specialists (Table 3). The performance of DeepSeeNet (accuracy=0.671; kappa=0.558) was superior to that of the retinal specialists (accuracy=0.599; kappa=0.467).

In addition, the performance of the individual sub-networks utilized in Fine-tuned DeepSeeNet (D-Net, P-Net, and LA-Net) was compared with that of retinal specialists (Table 4). Figure 2 displays receiver operator characteristic (ROC) curves for the individual sub-networks, with the average performance of the retinal specialists shown as single blue points. The performance of D-Net and P-net were superior to the performance of the retinal specialists in assessing large drusen and pigmentary abnormalities, respectively. The accuracy of LA-Net was similar to that of the retinal specialists in assessing the presence of late AMD, though its kappa was lower.

Figure 3 shows confusion matrices comparing the performance of Fine-tuned DeepSeeNet and the retinal specialists in grading AMD severity (with accuracy comparisons detailed in Table S1, available at www.aaojournal.org). These matrices depict the true versus the predicted AREDS Simplified Severity Scale scores of the 450 participants at baseline. The numbers of predictions are summarized with count values broken down by each class, indicating the accuracy and errors made by either DeepSeeNet or the retinal specialists. From Figure 3, it is seen that DeepSeeNet correctly classified scores 0-4 more often than the retinal specialists, while the retinal specialists correctly classified late AMD more often than DeepSeeNet.

Lastly, the performance of Fine-tuned DeepSeeNet was also compared on all images in the test set (accuracy=0.662; kappa=0.555) and images at study baseline (Table S2, available at www.aaojournal.org). We observed that the overall accuracy is at the study baseline are slightly better than overall data, however the kappas are same. While it is true that the distribution of AMD severity (for the testing cases) was on the slightly less severe side at baseline only, we do not consider this to have introduced ‘bias’, in the true meaning of the word, as the test cases were the same for the model as for the humans.

Interpretation

Although Fine-tuned DeepSeeNet demonstrated a relatively robust performance on classifying color fundus photographs according to AMD severity, the mechanics of this and other deep learning models are sometimes considered cryptic or lacking in transparency. Indeed, for this reason, deep learning models are often referred to as ‘black box’ entities. In order to improve transparency, in addition to creating models composed of sub-networks with overt purposes, we applied two additional techniques to aid interpretation of the results.

T-Distributed Stochastic Neighbor Embedding (t-SNE) Method

In this study, the internal features learned by Fine-tuned DeepSeeNet were studied using t-distributed Stochastic Neighbor Embedding (t-SNE; see Glossary), which is well suited for the visualization of high-dimensional datasets[51]. We first obtained the 128-dimensional vector of DeepSeeNet’s last dense layer and applied the t-SNE technique to reduce the vector into two dimensions for visualization (Figure 4). Figure 4 demonstrates that, for drusen, small/none drusen and large drusen were split across the medium drusen point cloud. The figure contains some points that are clustered with the wrong class, many of which are medium drusen and difficult to identify. For pigmentary abnormality and late AMD, presence and absence classes were separated clearly.

Saliency Method

The second method used to aid interpretation of the results towards model transparency was the saliency method. In order to visualize important areas in the color fundus images (i.e., those areas that contributed most towards classification), we applied image-specific class saliency maps to assess manually whether DeepSeeNet was concentrating on image areas that human experts would consider the most appropriate to predict AMD severity[52]. The saliency map is widely used to represent the visually dominant location in a given image, corresponding to the category of interest, by back-projecting the relevant features through the CNN. It helps highlight areas used by the deep learning algorithm for prediction and can also provide insight into misclassified images. For example, as seen in the ‘drusen’ category of Figure 5, the areas highlighted in the saliency maps are indeed areas with drusen that are visually apparent in the color fundus images. Similarly, in the ‘pigmentary changes’ and ‘late AMD’ categories in Figure 5, the areas highlighted in the saliency maps are visually confirmed to correspond with the relevant features in the corresponding color fundus images. However, although saliency maps aid interpretation by highlighting the dominant areas, they are limited in that they do not completely explain how the algorithm came to its final decision.

Discussion

The accuracy of Fine-Tuned DeepSeeNet was superior to that of human retinal specialists (accuracy 67% vs 60%), together with moderate agreement with the ground truth as indicated by the kappa score. If deep learning approaches were to support eye services in the future, comparisons of this kind (with demonstration of non-inferiority to human clinicians) would be very important, together with extensive validation across multiple and diverse image datasets. Interestingly, while the overall accuracy of Fine-tuned DeepSeeNet was superior, subgroup analysis showed that Fine-tuned DeepSeeNet classified participants with Severity Scale scores 0-4 correctly more often than the retinal specialists, while the retinal specialists classified late AMD correctly more often than Fine-Tuned DeepSeeNet (Figure 3). However, one important potential reason for the latter difference is that the number of images of late AMD that were available for model training was relatively low at 13.0% of the total training set (537 participants). We postulate that further training of Fine-tuned DeepSeeNet with larger numbers of late AMD images may improve its performance in this area.

Error analysis on misclassified images in the AREDS testing dataset

We considered that useful lessons might be learnt by careful examination of those instances where Fine-tuned DeepSeeNet made errors in the Severity Scale classification, particularly (as described above) in the case of late AMD (where its accuracy was lower than that of the retinal specialists). The matrices shown in Figure 3 demonstrate that, for actual Severity Scale scores of 0-4, in the large majority of cases, the score predicted by Fine-tuned DeepSeeNet was incorrect by 1 scale step only. We also examined those cases where Fine-tuned DeepSeeNet incorrectly classified a participant as having late AMD (score 5), and found that, in 50% of these cases, non-central GA was present in at least one eye. For the purposes of this study, non-central GA was not defined as late AMD, though recent studies have expanded the definition of late AMD to include non-central GA[7]. The misclassification of these images by our deep learning model suggest an inherent similarity between these groups of images.

Image quality also affected the accuracy of the deep learning model. Of the participants classified incorrectly by Fine-tuned DeepSeeNet as having late AMD, 25.0% had digital artifacts obscuring the fovea. In addition, image brightness affected the model accuracy. Participants with a pale retina, secondary to melanin loss in the RPE or digital artifacts, were more likely to be misclassified as having GA. In the future, we aim to address these problems by identifying color fundus photographs with inferior quality, either for exclusion or for additional processing.

Strengths, limitations, and future work

One current limitation of DeepSeeNet (at least in its present iteration) arises from the imbalance of cases that were available in the AREDS dataset used for its training, particularly the relatively low proportion of participants with late AMD. As described above, this is likely to have contributed to the relatively lower accuracy of DeepSeeNet in the classification of late AMD, i.e., through the performance of Late AMD-Net in the overall model. However, this limitation may potentially be addressed by further training using image datasets with a higher proportion of late AMD cases.

A limitation of this dataset includes the sole use of color fundus photographs as this was the only images obtained in a study that began in 1992. Multi-modal imaging would be desirable. Other imaging techniques such as optical coherence tomography and fundus autofluorescence images were not yet feasible or universally available. Future studies would benefit from inclusion such addition methods of imaging.

Another potential limitation lies in the reliance of DeepSeeNet on higher levels of image quality for accurate classification. Unlike in other studies[16,19], we did not perform extensive pre-processing of images, such as the detection of the outer boundaries of the retina or normalization of the color balance and local illumination. It is possible that the use of these techniques might have improved the accuracy of the model. However, we deliberately avoided extensive pre-processing in order to make our model as generalizable as possible.

We recommend further testing of our deep learning model, using other datasets of color fundus images. In addition, it would be interesting for future studies to compare the accuracy of the model against those of different groups of ophthalmologists (e.g. retinal specialists, general ophthalmologists, and trainee ophthalmologists). Indeed, a recent study on grader variability for diabetic retinopathy severity using color fundus photographs suggested that retinal specialists have a higher accuracy than that of general ophthalmologists[53]. In the current study, we therefore set the bar as high as possible for the deep learning model, as we considered that the retinal specialists might have accuracy as close as possible to that of the Reading Center gradings.

In conclusion, this study shows that DeepSeeNet performed patient-based AMD severity classification with a level of accuracy higher than a group of human retinal specialists. If these results are tested and validated by further reports of superiority across multiple datasets (ideally from different countries), it is possible that the integration of deep learning models into clinical practice might become increasingly acceptable to patients and ophthalmologists. In the future, deep learning models might support eye services by reducing the time and human expertise needed to classify retinal images and might lend themselves well (through telemedicine approaches) to improving care in geographical areas where current services are absent or limited. Although deep learning models are often considered ‘black box’ entities (owing to difficulties in understanding how algorithms make their predictions), we aimed to improve the transparency of DeepSeeNet by constructing it from sub-networks with clear purposes (e.g. drusen detection) and analyzing its outputs with saliency maps. These efforts to demystify deep learning models may help improve levels of acceptability to patients and adoption by ophthalmologists. We have also analyzed the performance of several distinct training strategies; lessons from these approaches may have applicability to the development of deep learning models for other retinal diseases, such as diabetic retinopathy, and even for image-based deep learning systems outside of ophthalmology.

Our new model utilizes deep learning in combination with a clinically useful, patient-based, AMD classification system that combines risk factors from both eyes to obtain a score for the patient. The deep learning model and data partition are publicly available (https://github.com/ncbi-nlp/DeepSeeNet). By making these available, we aim to maximize the transparency and reproducibility of this study, and to provide a benchmark method for the further refinement and development of methodologies. In addition, this deep learning model, trained on one of the largest publicly-available color fundus photograph repositories, may allow for future deep learning studies of other retinal diseases in which only smaller datasets are currently available.

In the future, we aim to improve the model by incorporating other information such as demographic, medical, and genetic data, potentially together with imaging data from other modalities. We also plan to evaluate our model on a new dataset from the second Age-Related Eye Disease Study sponsored by the National Eye Institute (AREDS2). In addition, we hope to investigate the combination of OCT-based and CFP-based deep learning models once each has been more highly validated individually. Taken together, we expect this study will contribute to the advancement and understanding of retinal disease and may ultimately enhance clinical decision-making.

Supplementary Material

Refer to Web version on PubMed Central for supplementary material.

Acknowledgments

Financial Support: Supported by the intramural program funds and contracts from the National Center for Biotechnology Information/National Library of Medicine/National Institutes of Health, the National Eye Institute/National Institutes of Health, Department of Health and Human Services, Bethesda Maryland (contract HHS-N-260-2005-00007-C; ADB contract NO1-EY-5-0007). Funds were generously contributed to these contracts by the following NIH institutes: Office of Dietary Supplements, National Center for Complementary and Alternative Medicine; National Institute on Aging; National Heart, Lung, and Blood Institute, and National Institute of Neurological Disorders and Stroke. The sponsor and funding organization participated in the design and conduct of the study; data collection, management, analysis and interpretation; and the preparation, review and approval of the manuscript.

Glossary

Adam optimizer

Adam is an optimization algorithm to update network weights. Different from classical optimization that maintains a single learning rate for all weight updates and the learning rate does not change during training, it computes adaptive learning rates for different parameters during the training[46].

Back-propagation

A method used in artificial neural networks to calculate a gradient that is needed in the calculation of the weights to be used in the network[54].

Convolutional neural network

A class of artificial neural network algorithms utilized in deep learning largely for image classification.

Deep learning

A subfield of machine learning in which explicit features are determined from the training data and do not require pre-specification by human domain experts.

Development set

A mutually exclusive set of images not utilized in the training set. These images are used for testing deep learning models, in order to evaluate their performance levels.

Epoch

A single pass through the entire training set.

Fine-tune

A process to take a neural network model that has already been trained for a given task, and make it perform a second task.

Fully-connected layer

A linear operation in which every output neuron has connections to all activations in the previous layer.

Hidden layer

The middle layer of a neural network, because its values are not observed in the training set.

ImageNet

An image database comprised of >14 million natural images and their corresponding labels. Due to the large number of labeled images, this dataset is often employed in deep learning techniques to pre-train models. In a process known as transfer learning, the first layers are trained with ImageNet to extract more primitive features from the images (e.g., edge detection).

Inception-v3

A convolutional neural network with the inception architecture for computer vision[43].

Layer

A container that usually receives weighted input, transforms it with a set of mostly non-linear functions, and then passes these values as output to the next layer.

Leaning rate

A hyper-parameter that controls how much the weights of deep neural network are adjusted with respect the loss gradient.

Multiclass classification

A classification task with more than two classes.

Multilayer perceptron

A class of feedforward artificial neural network that consists of at least one hidden layer.

Over-fitting

The production of an analysis that corresponds too closely or exactly to a particular set of data and may therefore fail to fit additional data or predict future observations reliably.

Saliency map

The saliency map is computed for an input image and a given output class It tells us which pixels in the image contribute most to the model’s classification of that class. Specifically, we first computed the gradient of a given label with respect to the input image. The gradient, by definition, points in the direction of the greatest rate of class changes with respect to a small change in the input images. That small region of changes in the input image, thereby, contributes most and is highlighted in the saliency map.

Stochastic gradient descent

An iterative method for optimizing the objective function in machine learning.

Training

A data-driven approach requiring tens of thousands of labeled images for the training set.

Training set

The set of images used for training a deep learning model. The network then predicts the category of each image and compares it with known “ground truth” labels. The parameters in the network are then optimized to improve the model’s predictive ability, in a process known as back-propagation.

Transfer learning

The process of training a deep learning model on a large set of data, such that the model’s weights are optimized as learned features. These weights are then “transferred” to a new neural network to allow for more efficient training of the model on a new training set (often smaller in size).

t-SNE

t-SNE is a technique used to visualize and explore complex datasets (particularly those with high-dimensional features) in a low-dimensional space. In our case, we use it to creates a two-dimensional map by assigning a location to each datapoint (each retinal image). The locations are decided by probability distributions, such that datapoints that are similar across high-dimensional features end up close to each other, and datapoints that are dissimilar end up far apart. As a result, t-SNE plots often seem to display clusters (e.g. the cluster for large drusen, in this case), where the datapoints in the cluster all have relatively similar features. It can therefore be used to help the classification process, and in the visual inspection and exploration of results from deep learning experiments[55]

Weights

Learnable parameters of the deep learning model.

References

1. Quartilho A, Simkiss P, Zekite A, Xing W, Wormald R, Bunce C. Leading causes of certifiable visual loss in England and Wales during the year ending 31 March 2013. Eye (Lond). 2016;30(4): 602–607. [PubMed: 26821759]
2. Congdon N, O'Colmain B, Klaver CC, et al. Causes and prevalence of visual impairment among adults in the United States. Archives of ophthalmology. 2004;122(4):477–485. [PubMed: 15078664]
3. Wong WL, Su X, Li X, et al. Global prevalence of age-related macular degeneration and disease burden projection for 2020 and 2040: a systematic review and meta-analysis. Lancet Glob Health. 2014;2(2):e106–116. [PubMed: 25104651]
4. Rudnicka AR, Jarrar Z, Wormald R, Cook DG, Fletcher A, Owen CG. Age and gender variations in age-related macular degeneration prevalence in populations of European ancestry: a meta-analysis. Ophthalmology. 2012;119(3):571–580. [PubMed: 22176800]
5. Fritsche LG, Fariss RN, Stambolian D, Abecasis GR, Curcio CA, Swaroop A. Age-related macular degeneration: genetics and biology coming together. Annu Rev Genomics Hum Genet. 2014;15:151–171. [PubMed: 24773320]

6. Ratnapriya R, Chew EY. Age-related macular degeneration-clinical review and genetics update. Clin Genet. 2013;84(2):160–166. [PubMed: 23713713]

7. Ferris FL, 3rd, Wilkinson CP, Bird A, et al. Clinical classification of age-related macular degeneration. Ophthalmology. 2013;120(4):844–851. [PubMed: 23332590]

8. Group A-REDSR. A simplified severity scale for age-related macular degeneration: AREDS Report No. 18. Archives of ophthalmology. 2005;123(11):1570–1574. [PubMed: 16286620]

9. Ching T, Himmelstein DS, Beaulieu-Jones BK, et al. Opportunities and obstacles for deep learning in biology and medicine. Journal of The Royal Society Interface. 2018;15(141).

10. Wang X, Peng Y, Lu L, Lu Z, Bagheri M, Summers RM. Chestx-ray8: Hospital-scale chest x-ray database and benchmarks on weakly-supervised classification and localization of common thorax diseases. 2017 IEEE Conference on Computer Vision and Pattern Recognition (CVPR) 2017:3462–3471.

11. Wang X, Peng Y, Lu L, Lu Z, Summers RM. TieNet: Text-Image Embedding Network for Common Thorax Disease Classification and Reporting in Chest X-rays. IEEE Conference on Computer Vision and Pattern Recognition (CVPR) 2018.

12. Banerjee I, Madhavan S, Goldman RE, Rubin DL. Intelligent Word Embeddings of Free- Text Radiology Reports. arXiv preprint arXiv:171106968. 2017.

13. Esteva A, Kuprel B, Novoa RA, et al. Dermatologist-level classification of skin cancer with deep neural networks. Nature. 2017;542(7639):115–118. [PubMed: 28117445]

14. Ehteshami Bejnordi B, Veta M, Johannes van Diest P, et al. Diagnostic Assessment of Deep Learning Algorithms for Detection of Lymph Node Metastases in Women With Breast Cancer. Jama. 2017;318(22):2199–2210. [PubMed: 29234806]

15. Lehman CD, Wellman RD, Buist DS, et al. Diagnostic Accuracy of Digital Screening Mammography With and Without Computer-Aided Detection. JAMA internal medicine. 2015;175(11):1828–1837. [PubMed: 26414882]

16. Grassmann F, Mengelkamp J, Brandl C, et al. A Deep Learning Algorithm for Prediction of Age-Related Eye Disease Study Severity Scale for Age-Related Macular Degeneration from Color Fundus Photography. Ophthalmology. 2018.

17. Kermany DS, Goldbaum M, Cai W, et al. Identifying Medical Diagnoses and Treatable Diseases by Image-Based Deep Learning. Cell. 2018;172(5):1122–1131 e1129. [PubMed: 29474911]

18. Burlina P, Freund DE, Joshi N, Wolfson Y, Bressler NM. Detection of age-related macular degeneration via deep learning. 2016:184–188.

19. Burlina PM, Joshi N, Pekala M, Pacheco KD, Freund DE, Bressler NM. Automated Grading of Age-Related Macular Degeneration From Color Fundus Images Using Deep Convolutional Neural Networks. JAMA ophthalmology. 2017;135(11):1170–1176. [PubMed: 28973096]

20. Lam C, Yu C, Huang L, Rubin D. Retinal Lesion Detection With Deep Learning Using Image Patches. Investigative ophthalmology & visual science. 2018;59(1):590–596. [PubMed: 29372258]

21. Lee CS, Tyring AJ, Deruyter NP, Wu Y, Rokem A, Lee AY. Deep-learning based, automated segmentation of macular edema in optical coherence tomography. Biomedical optics express. 2017;8(7):3440–3448. [PubMed: 28717579]

22. Choi JY, Yoo TK, Seo JG, Kwak J, Um TT, Rim TH. Multi-categorical deep learning neural network to classify retinal images: A pilot study employing small database. PLoS One. 2017;12(11):e0187336. [PubMed: 29095872]

23. Gargeya R, Leng T. Automated Identification of Diabetic Retinopathy Using Deep Learning. Ophthalmology. 2017;124(7):962–969. [PubMed: 28359545]

24. Gulshan V, Peng L, Coram M, et al. Development and Validation of a Deep Learning Algorithm for Detection of Diabetic Retinopathy in Retinal Fundus Photographs. Jama. 2016;316(22):2402–2410. [PubMed: 27898976]

25. Raju M, Pagidimarri V, Barreto R, Kadam A, Kasivajjala V, Aswath A. Development of a Deep Learning Algorithm for Automatic Diagnosis of Diabetic Retinopathy. Studies in health technology and informatics. 2017;245:559–563. [PubMed: 29295157]

26. Takahashi H, Tampo H, Arai Y, Inoue Y, Kawashima H. Applying artificial intelligence to disease staging: Deep learning for improved staging of diabetic retinopathy. PLoS One. 2017;12(6):e0179790. [PubMed: 28640840]

27. Ting DSW, Cheung CY, Lim G, et al. Development and Validation of a Deep Learning System for Diabetic Retinopathy and Related Eye Diseases Using Retinal Images From Multiethnic Populations With Diabetes. Jama. 2017;318(22):2211–2223. [PubMed: 29234807]

28. Asaoka R, Murata H, Iwase A, Araie M. Detecting Preperimetric Glaucoma with Standard Automated Perimetry Using a Deep Learning Classifier. Ophthalmology. 2016;123(9):1974–1980. [PubMed: 27395766]

29. Cerentini A, Welfer D, Cordeiro d'Ornellas M, Pereira Haygert CJ, Dotto GN. Automatic Identification of Glaucoma Using Deep Learning Methods. Studies in health technology and informatics. 2017;245:318–321. [PubMed: 29295107]

30. Muhammad H, Fuchs TJ, De Cuir N, et al. Hybrid Deep Learning on Single Wide-field Optical Coherence tomography Scans Accurately Classifies Glaucoma Suspects. J Glaucoma. 2017;26(12):1086–1094. [PubMed: 29045329]

31. Brown JM, Campbell JP, Beers A, et al. Automated Diagnosis of Plus Disease in Retinopathy of Prematurity Using Deep Convolutional Neural Networks. JAMA ophthalmology. 2018.

32. Matsuba S, Tabuchi H, Ohsugi H, et al. Accuracy of ultra-wide-field fundus ophthalmoscopy-assisted deep learning, a machine-learning technology, for detecting age-related macular degeneration. Int Ophthalmol. 2018.

33. Treder M, Lauermann JL, Eter N. Automated detection of exudative age-related macular degeneration in spectral domain optical coherence tomography using deep learning. Graefe's archive for clinical and experimental ophthalmology = Albrecht von Graefes Archiv fur klinische und experimentelle Ophthalmologie. 2018;256(2):259–265.

34. Burlina PM, Joshi N, Pacheco KD, Freund DE, Kong J, Bressler NM. Use of Deep Learning for Detailed Severity Characterization and Estimation of 5-Year Risk Among Patients With Age-Related Macular Degeneration. JAMA ophthalmology. 2018.

35. Burlina P, Pacheco KD, Joshi N, Freund DE, Bressler NM. Comparing humans and deep learning performance for grading AMD: A study in using universal deep features and transfer learning for automated AMD analysis. Computers in biology and medicine. 2017;82:80–86. [PubMed: 28167406]

36. Karri SP, Chakraborty D, Chatterjee J. Transfer learning based classification of optical coherence tomography images with diabetic macular edema and dry age-related macular degeneration. Biomedical optics express. 2017;8(2):579–592. [PubMed: 28270969]

37. De Fauw J, Ledsam JR, Romera-Paredes B, et al. Clinically applicable deep learning for diagnosis and referral in retinal disease. Nature medicine. 2018;24(9):1342–1350.

38. Srinivasan PP, Kim LA, Mettu PS, et al. Fully automated detection of diabetic macular edema and dry age-related macular degeneration from optical coherence tomography images. Biomedical optics express. 2014;5(10):3568–3577. [PubMed: 25360373]

39. Farsiu S, Chiu SJ, O'Connell RV, et al. Quantitative classification of eyes with and without intermediate age-related macular degeneration using optical coherence tomography. Ophthalmology. 2014;121(1):162–172. [PubMed: 23993787]

40. Marmor MF, Ravin JG. Fluorescein angiography: insight and serendipity a half century ago. Archives of ophthalmology. 2011;129(7):943–948. [PubMed: 21746986]

41. Group A-REDSR. The Age-Related Eye Disease Study system for classifying age-related macular degeneration from stereoscopic color fundus photographs: the Age-Related Eye Disease Study Report Number 6. American journal of ophthalmology. 2001;132(5):668–681. [PubMed: 11704028]

42. LeCun Y. Generalization and network design strategies. Connectionism in perspective. 1989:143–155.

43. Szegedy C, Vanhoucke V, Ioffe S, Shlens J, Wojna Z. Rethinking the inception architecture for computer vision. Proceedings of the IEEE Conference on Computer Vision and Pattern Recognition 2016:2818–2826.

44. Abadi M, Agarwal A, Barham P, et al. TensorFlow: Large-Scale Machine Learning on Heterogeneous Distributed Systems. arXiv. 2016.

45. Chollet F, others. Keras. https://keras.io, 2015.

46. Kingma DP, Ba J. Adam: A method for stochastic optimization. International Conference on Learning Representations (ICLR). 2015:1–15.

47. Cohen J A Coefficient of Agreement for Nominal Scales. Educational and Psychological Measurement. 2016;20(1):37–46.

48. Cohen J Multiple regression as a general data-analytic system. Psychological Bulletin. 1968;70(6, Pt.1):426–443.

49. Landis JR, Koch GG. The measurement of observer agreement for categorical data. Biometrics. 1977;33(1):159–174. [PubMed: 843571]

50. Poplin R, Varadarajan AV, Blumer K, et al. Prediction of cardiovascular risk factors from retinal fundus photographs via deep learning. Nature Biomedical Engineering. 2018;2(3):158–164.

51. Van Der Maaten L Accelerating t-SNE using tree-based algorithms. Journal of machine learning research. 2014;15(1):3221–3245.

52. Simonyan K, Vedaldi A, Zisserman A. Deep inside convolutional networks: Visualising image classification models and saliency maps. arXiv preprint arXiv:13126034. 2013.

53. Krause J, Gulshan V, Rahimy E, et al. Grader Variability and the Importance of Reference Standards for Evaluating Machine Learning Models for Diabetic Retinopathy. Ophthalmology. 2018.

54. Goodfellow I, Bengio Y, Courville A. Deep Learning. MIT Press; 2016.

55. Maaten L, Hinton G. Visualizing data using t-SNE. Journal of machine learning research. 2008;9(11):2579–2605.

A novel deep learning model developed to automatically classify patient-based age-related macular degeneration severity from bilateral color fundus images achieved comparable performance to that of retinal specialist ophthalmologists.

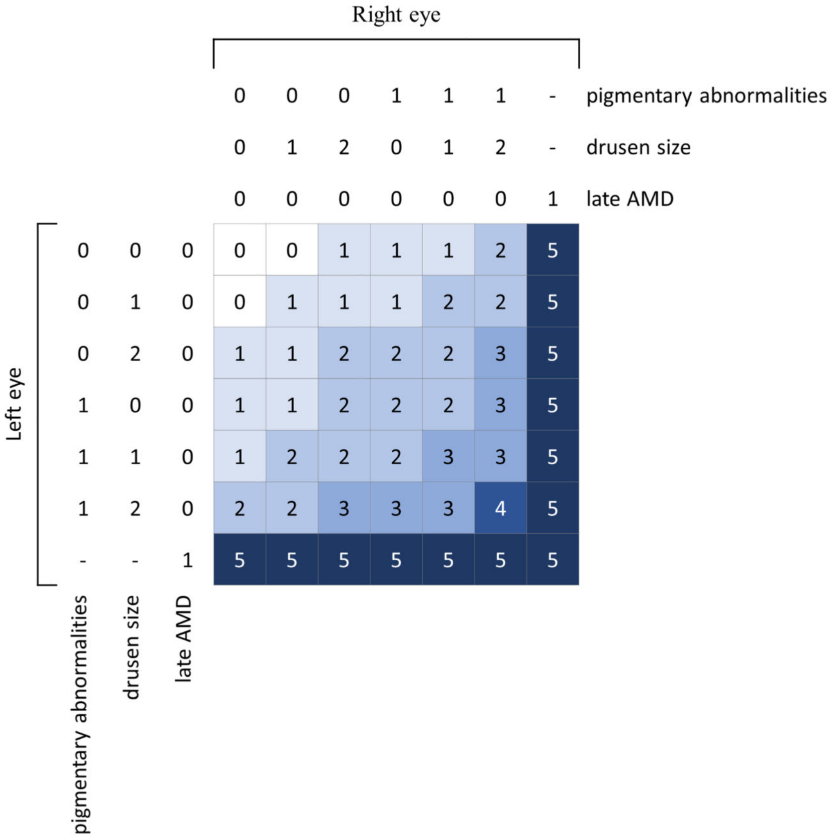

Left eye			Right eye							
			0	0	0	1	1	1	-	pigmentary abnormalities
			0	1	2	0	1	2	-	drusen size
			0	0	0	0	0	0	1	late AMD
0	0	0	0	0	1	1	1	2	5	
0	1	0	0	1	1	1	2	2	5	
0	2	0	1	1	2	2	2	3	5	
1	0	0	1	1	2	2	2	3	5	
1	1	0	1	2	2	2	3	3	5	
1	2	0	2	2	3	3	3	4	5	
-	-	1	5	5	5	5	5	5	5	
pigmentary abnormalities	drusen size	late AMD								

Figure 1.

Scoring schematic for participants with and without late age-related macular degeneration. Pigmentary abnormalities- 0-no, 1-yes; drusen size- 0-small or none, 1-medium, 2-large; late AMD- 0-no, 1-yes.

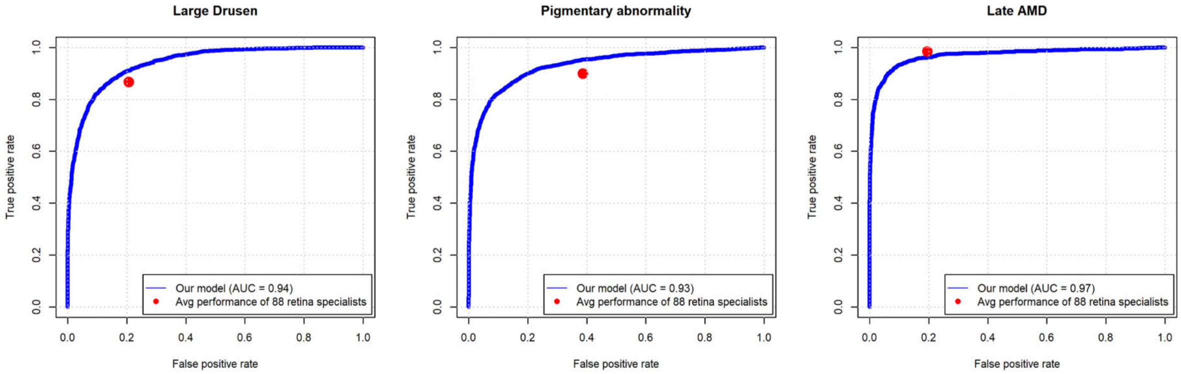

Figure 2.

Receiver operating characteristic curves for large drusen, pigment abnormalities, and late AMD classification. Retinal specialists performance levels are represented as a single blue point.

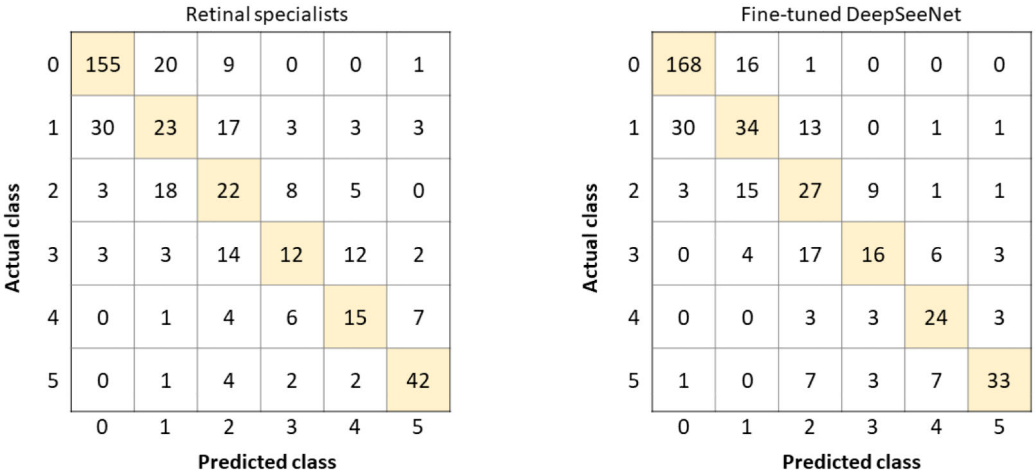

Retinal specialists

Actual class \ Predicted class	0	1	2	3	4	5
0	155	20	9	0	0	1
1	30	23	17	3	3	3
2	3	18	22	8	5	0
3	3	3	14	12	12	2
4	0	1	4	6	15	7
5	0	1	4	2	2	42

Fine-tuned DeepSeeNet

Actual class \ Predicted class	0	1	2	3	4	5
0	168	16	1	0	0	0
1	30	34	13	0	1	1
2	3	15	27	9	1	1
3	0	4	17	16	6	3
4	0	0	3	3	24	3
5	1	0	7	3	7	33

Figure 3.

Confusion matrices comparing retinal specialists' performance with that of DeepSeeNet based on the test set values. The rows and columns of each matrix are the Scale scores (0-5).

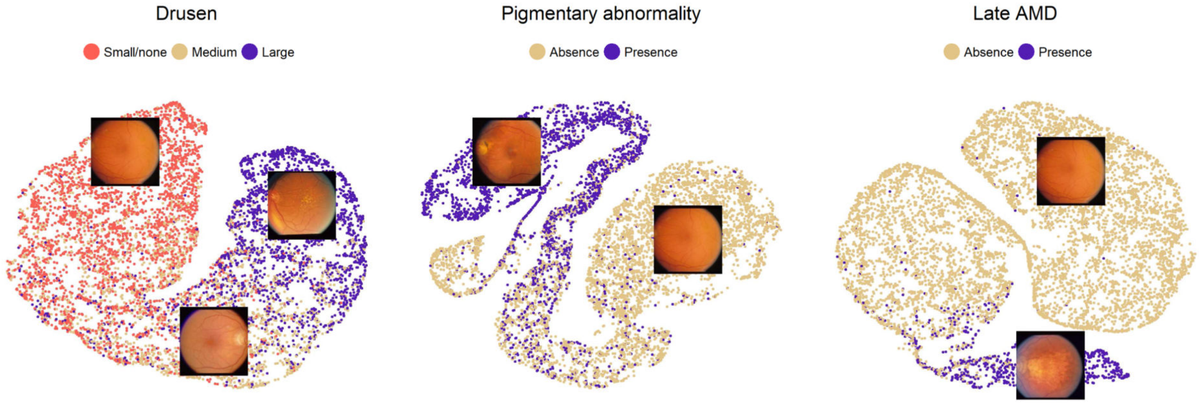

Figure 4.

t-SNE visualization of the last hidden layer representation for each sub-network of DeepSeeNet. Each point represents a fundus image. Different colors represent the different classes of the respective risk factor or late AMD.

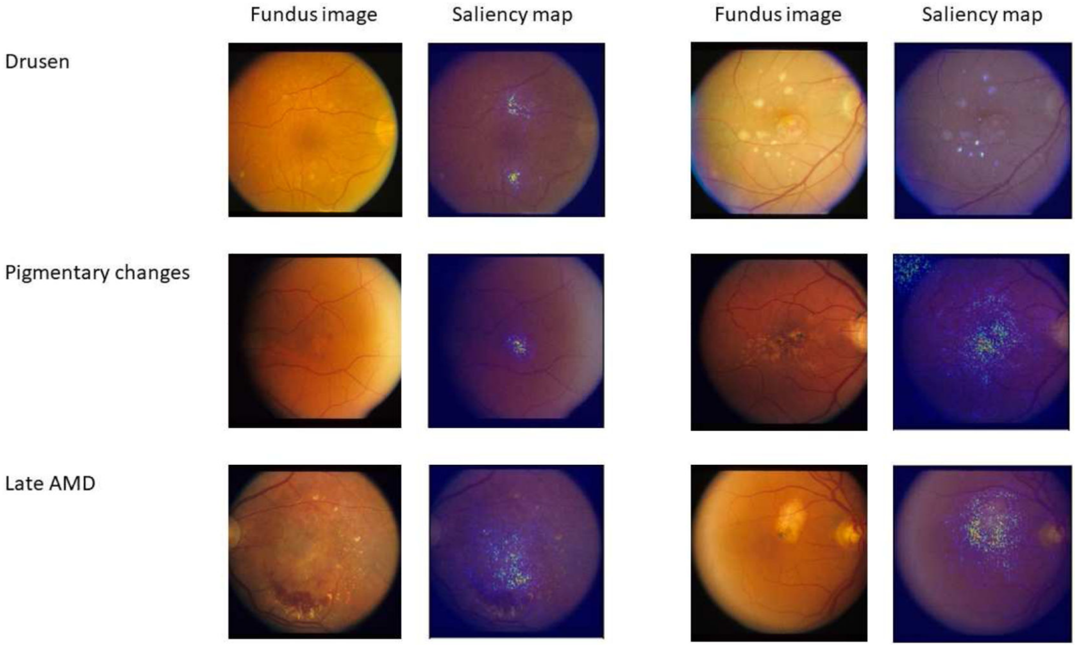

Figure 5.
Image-specific class saliency maps that highlight the macular region for color fundus photographs with large drusen, pigmentary abnormalities, and late AMD.

Table 1.

Summary of AREDS participants according to AREDS Simplified Severity Scale scores at study baseline (by Reading Centre grading).

AREDS Simplified Severity Scale Score	No. of Participants (% Total)			
	Training		Testing	
0	1,258	(30.7)	185	(41.1)
1	653	(15.9)	79	(17.6)
2	461	(11.3)	56	(12.4)
3	303	(7.4)	46	(10.2)
4	279	(6.8)	33	(7.3)
5	537	(13.1)	51	(11.3)
Total participants	4,099	(100.0)	450	(100.0)

Table 2.

Number of color fundus images in the training and testing sets stratified by risk factors and late AMD categorization.

Risk factors	Number of Fundus Images (% Total)			
	Training (all visits)		Testing (baseline)	
Drusen				
Small/none	23,625	(40.5)	395	(43.9)
Medium	16,020	(27.4)	206	(22.9)
Large	18,757	(32.1)	299	(33.2)
Pigmentary abnormalities				
No	36,712	(62.9)	631	(70.1)
Yes	21,690	(37.1)	269	(29.9)
Late AMD				
No	50,800	(87.0)	849	(94.3)
Yes	7,602	(13.0)	51	(5.7)
Total images	58,402	(100.0)	900	(100.0)

Table 3.

Performance of Fine-tuned DeepSeeNet compared to retinal specialists; on classifying AREDS Simplified Severity Scale scores from color fundus photographs.

	Fine-tuned DeepSeeNet	**Retinal specialist**
	(95% CI)	**(95% CI)**
Overall accuracy	0.671 (0.670, 0.672)	0.599 (0.598, 0.600)
Sensitivity	0.590 (0.589, 0.591)	0.512 (0.511, 0.513)
Specificity	0.930 (0.930, 0.930)	0.916 (0.916, 0.916)
Kappa	0.558 (0.557, 0.560)	0.467 (0.466, 0.468)

Table 4.

Performance of risk factor prediction (retinal specialists versus individual sub-network models).

	Drusen		Pigmentary Changes		Late AMD	
	Retinal specialist	**D-Net**	**Retinal specialist**	**P-Net**	**Retinal specialist**	**LA-Net**
Overall accuracy (95% CI)	0.696 (0.695, 0.697)	0.742 (0.741, 0.742)	0.813 (0.813, 0.814)	0.890 (0.889, 0.890)	0.973 (0.973, 0.973)	0.967 (0.967, 0.967)
Sensitivity (95% CI)	0.635 (0.634, 0.636)	0.718 (0.717, 0.719)	0.615 (0.613, 0.616)	0.732 (0.731, 0.733)	0.801 (0.798, 0.805)	0.627 (0.626, 0.632)
Specificity (95% CI)	0.842 (0.842, 0.843)	0.871 (0.871, 0.872)	0.898 (0.898, 0.899)	0.957 (0.957, 0.957)	0.983 (0.983, 0.984)	0.987 (0.987, 0.987)
Kappa (95% CI)	0.517 (0.516, 0.518)	0.601 (0.600, 0.602)	0.535 (0.533, 0.536)	0.723 (0.722, 0.724)	0.754 (0.751, 0.757)	0.663 (0.660, 0.665)

Abbreviations: D-Net- Drusen-Net, which classifies drusen into three size categories (small/none, medium, and large); P-Net- Pigment-Net, which detects the presence or absence of any pigmentary abnormality consistent with AMD (hypopigmentation or hyperpigmentation); LA-Net- Late AMD-Net, which detects the presence or absence of late AMD (neovascular AMD or central GA).